https://doi.org/10.5194/egusphere-2024-2698
Preprint. Discussion started: 18 September 2024

Theoretical Framework for Measuring Cloud Effective Supersaturation Fluctuations with an Advanced Optical System

Ye Kuang[1], Jiangchuan Tao[1], Hanbin Xu[2], Li Liu[3], Pengfei Liu[4], Wanyun Xu[5], Weiqi Xu[6], Yele Sun[6], Chunsheng Zhao[7]

[1] Institute for Environmental and Climate Research, College of Environment and Climate, Jinan University, Guangzhou, Guangdong, China

[2] Experimental Teaching Center, Sun Yat-Sen University, Guangzhou, China

[3] Key Laboratory of Regional Numerical Weather Prediction, Institute of Tropical and Marine Meteorology, China Meteorological Administration, Guangzhou, China.

[4] School of Earth and Atmospheric Sciences, Georgia Institute of Technology, Atlanta, GA, USA

[5] State Key Laboratory of Severe Weather, Key Laboratory for Atmospheric Chemistry, Institute of Atmospheric Composition, Chinese Academy of Meteorological Sciences, Beijing, China

[6] State Key Laboratory of Atmospheric Boundary Layer Physics and Atmospheric Chemistry, Institute of Atmospheric Physics, Chinese Academy of Sciences, Beijing, China.

[7] Department of Atmospheric and Oceanic Sciences, School of Physics, Peking University, Beijing, China.

Correspondence: Ye Kuang (kuangye@jnu.edu.cn)

https://doi.org/10.5194/egusphere-2024-2698
Preprint. Discussion started: 18 September 2024

Abstract

Supersaturation is crucial in cloud physics, determining aerosol activation and influencing cloud droplet size distributions, yet its measurement remains challenging and poorly constrained. This study proposes a theoretical framework to simultaneously observe critical activation diameter and hygroscopicity of activated aerosols through direct measurements of scattering and water induced scattering enhancement of interstitial and activated aerosols, enabling effective supersaturation measurements. Advanced optical systems based on this framework allows minute- to second-level effective supersaturation measurements, capturing fluctuations vital to cloud microphysics. Although currently limited to clouds with supersaturations below ~0.2% due to small scattering signals from sub-100 nm aerosols, advancements in optical sensors could extend its applicability. Its suitability for long-term measurements allows for climatological studies of fogs and mountain clouds. When equipped with aerial vehicles, the system could also measure aloft clouds. Therefore, the proposed theory serving a valuable way for both short-term and long-term cloud microphysics and aerosol-cloud interaction studies.

https://doi.org/10.5194/egusphere-2024-2698
Preprint. Discussion started: 18 September 2024

1. Introduction

Clouds and fogs play critical roles in weather patterns and climate change, influencing both precipitation and the radiative balance of the Earth's atmosphere. As such, they are central to accurate weather and climate predictions. Despite their importance, representing clouds accurately in atmospheric models remains a significant challenge (Seinfeld et al., 2016). Supersaturation, defined as the difference between the actual water vapor pressure (e) and the saturation vapor pressure (es) which is typically expressed as a dimensionless quantity (e−es)/es, is a key parameter that links aerosols to clouds through the process of aerosol activation, making it fundamental to cloud physics (Seinfeld and Pandis, 2016). Despite its importance, supersaturation is difficult to measure and remains poorly understood and constrained (Yang et al., 2019). Previous studies have highlighted that other than the mean supersaturation, supersaturation fluctuations also play critical roles in aerosol activation and cloud droplet growth, ultimately influencing the evolution of cloud droplet size distributions (Kaufman and Tanré, 1994;Sardina et al., 2015;Chandrakar et al., 2018;Chandrakar et al., 2020;Shaw et al., 2020). For instance, cloud chamber experiments have shown that supersaturation fluctuations promote aerosol activation and enhance aerosol activity (Shawon et al., 2021;Anderson et al., 2023), particularly when the magnitude of these fluctuations is comparable to the mean supersaturation (Prabhakaran et al., 2020). Both experimental and theoretical analyses suggest that supersaturation fluctuations can broaden cloud droplet size distributions (Chandrakar et al., 2016;Abade et al., 2018;Saito et al., 2019).

Supersaturation fluctuations arise not only from turbulent variations in the temperature and vapor pressure fields but also from the growth and evaporation of droplets, which drive mass and heat exchange between droplets and the surrounding air. Field measurements have demonstrated that the supersaturation is indeed a fluctuating quantity (Ditas et al., 2012;Siebert and Shaw, 2017). However, as noted by Shaw et al. (2020), measuring supersaturation remains a formidable challenge due to its extreme sensitivity to variations in e and temperature. Currently, cloud and fog supersaturation are typically retrieved from aerosol activation measurements (Ditas et al., 2012) or estimated from vertical velocity measurements (Siebert and Shaw, 2017). Direct measurements of water vapor pressure and temperature are generally used to estimate supersaturation fluctuations but do not provide precise direct supersaturation measurements (Ditas et al., 2012;Siebert and Shaw, 2017). Supersaturation parameterizations based on vertical velocity are common in models (Abdul-Razzak et al., 1998), while field measurements often rely on aerosol activation data to investigate supersaturation fluctuations and evolutions in clouds and fogs (Ditas et al., 2012;Hammer et al., 2014;Shen et al., 2018;Mazoyer et al.,

https://doi.org/10.5194/egusphere-2024-2698
Preprint. Discussion started: 18 September 2024

2019;Zíková et al., 2020;Wainwright et al., 2021;Kuang et al., 2024). In addition, supersaturations were also estimated using the closure between cloud droplet number and cloud condensation nuclei (CCN) measurements at various supersaturations (Yum et al., 1998;Sanchez et al., 2016;Sanchez et al., 2021;Saliba et al., 2023).

In summary, direct measurements of water vapor pressure and temperature are essential for quantifying supersaturations; however, they are nearly impossible with current technologies. Supersaturation measurements from aerosol and cloud microphysics monitoring often reflect an effective supersaturation that drives aerosol activation, which is indeed critical in cloud physics. The complexity of cloud formation and evolution and the central role of supersaturation in these processes underscore the need for precise measurement and representation of supersaturation. Advancements in measuring and understanding supersaturation are essential for improving the accuracy of models and reducing uncertainties in weather and climate predictions. In this study, we propose a theoretical framework for using optical methods to observe effective supersaturations based on aerosol activation in clouds and preliminarily validated utilizing data obtained from field campaigns. The feasibility of employing an advanced optical system to measure supersaturation fluctuations were also explored and discussed.

2. Methods and Materials

2.1 Observing effective supersaturations on the basis of κ-Köhler theory

Fluctuations in supersaturation mean that the effective supersaturation, which directly affects aerosol activation, differs from the mean supersaturation. The κ-Köhler theory provides a framework for deriving effective supersaturation from aerosol activation measurements in clouds (Petters and Kreidenweis, 2007):

$$S = \frac{D^3 - {D_d}^3}{D^3 - {D_d}^3(1-\kappa)} \cdot \exp\left(\frac{4\sigma_{s/a} \cdot M_{water}}{R \cdot T \cdot D_p \cdot g \cdot \rho_w}\right) \quad (1)$$

where S is the saturation ratio, S-1 represents supersaturation, D is the droplet diameter, D_d is the dry diameter, $\sigma_{s/a}$ is the surface tension of solution/air interface, T is the temperature, M_{water} is the molecular weight of water, R is the universal gas constant, ρ_w is the density of water, and κ is the hygroscopicity parameter. The κ-Köhler theory tells that if the critical diameter of aerosol activation (D_a) and corresponding aerosol hygroscopicity parameter κ are known, the surrounding

https://doi.org/10.5194/egusphere-2024-2698
Preprint. Discussion started: 18 September 2024

supersaturation can be retrieved based on air temperature measurements and by assuming $\sigma_{s/a}$ the surface tension of water (as shown in Fig.S1a).

However, the simultaneous measurements of D_a and κ of activated aerosols with diameters around D_a are indeed challenging. The direct measurements of size-resolved activation ratio (AR) in clouds are essential for D_a retrievals through the following equation:

$$AR(\mathrm{D_p}) = \frac{\mathrm{MAF}}{2}\left(1+\mathrm{erf}\left(\frac{\mathrm{D_p}-\mathrm{D_a}}{\sqrt{2}\sigma}\right)\right) \qquad (2)$$

Where $\mathrm{D_p}$ is the particle diameter, MAF is the maximum activation fraction and $\mathrm{D_a}$ is critical activation diameter, σ is associated with the slope of the curve near $\mathrm{D_a}$. This formula was previously proposed by Rose et al. (2008) to fit the AR measurements and widely used in AR parameterizations (Tao et al., 2018b). Therefore, it typically requires a unique inlet system and a suite of instruments that measure the aerosol size distribution of both interstitial and total aerosol populations (Hammer et al., 2014;Zíková et al., 2020). Consequently, this is rarely done, even in ground fog measurements. Instead, D_a was usually estimated from aerosol measurements and fog droplet size distributions measurements which indirectly provides the number concentrations of activated aerosols therefore could be used in retrieving D_a through assuming that all aerosols larger than D_a are activated (Mazoyer et al., 2019;Wainwright et al., 2021;Shen et al., 2018) which brings uncertainty in D_a derivations due to that the maximum activation fraction of aerosols larger than D_a does not equal to unit although usually very close to (Tao et al., 2018b). For the effective supersaturation measured in aloft clouds, the aerosol number size distributions inside and outside the cloud as well as cloud droplet number concentrations were used by Ditas et al. (2012) to derive D_a, and other approaches were also used (Gong et al., 2023). The κ values were usually retrieved from size-resolved cloud condensation nuclei measurements under certain supersaturations (Hammer et al., 2014;Mazoyer et al., 2019) or from growth factor measurements (Wainwright et al., 2021) or sometime assumed due to the lack of measurements. The κ of activated aerosols were not directly measured in these studies due to the difficulty of the direct sampling of activated aerosols as well as subsequent hygroscopicity measurements.

2.2 Field measurements

Kuang et al. [2024] developed an advanced aerosol-cloud sampling system designed to measure fog and cloud activation processes. This compact, integrated system can automatically switch between different inlets, including PM_1 (particles and droplets with an aerodynamic diameter < 1 μm), $PM_{2.5}$

https://doi.org/10.5194/egusphere-2024-2698
Preprint. Discussion started: 18 September 2024

(particles and droplets with an aerodynamic diameter < 2.5 μm) impactor, and Total Suspended Particles (TSP, encompassing all particles and droplets) (as shown in Fig. S2). When combined with instruments that measure aerosol physical, optical, and chemical properties, this system is well-suited for investigating cloud microphysics and chemistry. It was utilized in the AQ-SOFAR campaign, dedicated to studying AQueous Secondary aerOsol formation in Fogs and Aerosols and their Radiative effects in the North China Plain (Kuang et al., 2024).

During this campaign, several radiation fog events were observed, enabling the measurement of size-resolved AR curves, aerosol hygroscopicity as well as chemical compositions of interstitial and activated aerosols within fogs. These measurements provided insights into the evolution of supersaturations (Kuang et al., 2024). Notably, aerosol hygroscopicity was determined using a humidified nephelometer system, located downstream of the inlet system. This system measured multiwavelength scattering coefficients (450 nm, 525 nm, 635 nm) under both nearly dry (RH<20%) and humid conditions (RH~84%), offering aerosol hygroscopicity data based on the optical theory proposed by Kuang et al. (2017). The size-resolved AR curves and aerosol chemical compositions were obtained through the aerosol size distribution and the aerosol mass spectrometry measurements downstream of the inlet system. A schematic of the inlet system and associated instruments is provided in Fig. S1. Further details about the entire experimental setup, size-resolved AR calculations as well as data analysis about mass spectrometer measurements can be found in Kuang et al. (2024).

3. Theoretical Framework and Concept Design of the Advanced Optical System

3.1 Theory of Observing Critical Activation Diameter Using Scattering Measurements

The typical shape of size-resolved AR curves observed in atmospheric fogs and clouds is illustrated in Fig. 1a (Ditas et al., 2012;Hammer et al., 2014;Zíková et al., 2020;Wainwright et al., 2021;Kuang et al., 2024). In clouds, aerosols can be classified as either activated aerosols, which form cloud droplets, or inactivated aerosols, which remain as interstitial aerosols. The critical diameter that distinguishes interstitial aerosols from cloud or fog droplets varies depending on the supersaturation (Kuang et al., 2024). A diameter of 2.5 μm is typically suitable for surface fogs with relatively lower supersaturations (<0.1%), while 1 μm is more appropriate for aloft clouds with higher supersaturations (>0.1%) (Mazoyer et al., 2019;Kuang et al., 2024;Lu et al., 2020). The typical AR curve shows that most aerosols larger than D_a are activated, while most smaller aerosols remain inactivated. As a result, the scattering properties, such as size-resolved scattering coefficients (Fig.1a), the scattering Ångström

https://doi.org/10.5194/egusphere-2024-2698
Preprint. Discussion started: 18 September 2024

178 exponent (SAE) and its wavelength dependence, which are directly related to aerosol size distribution,
179 differ significantly between interstitial and activated aerosols.

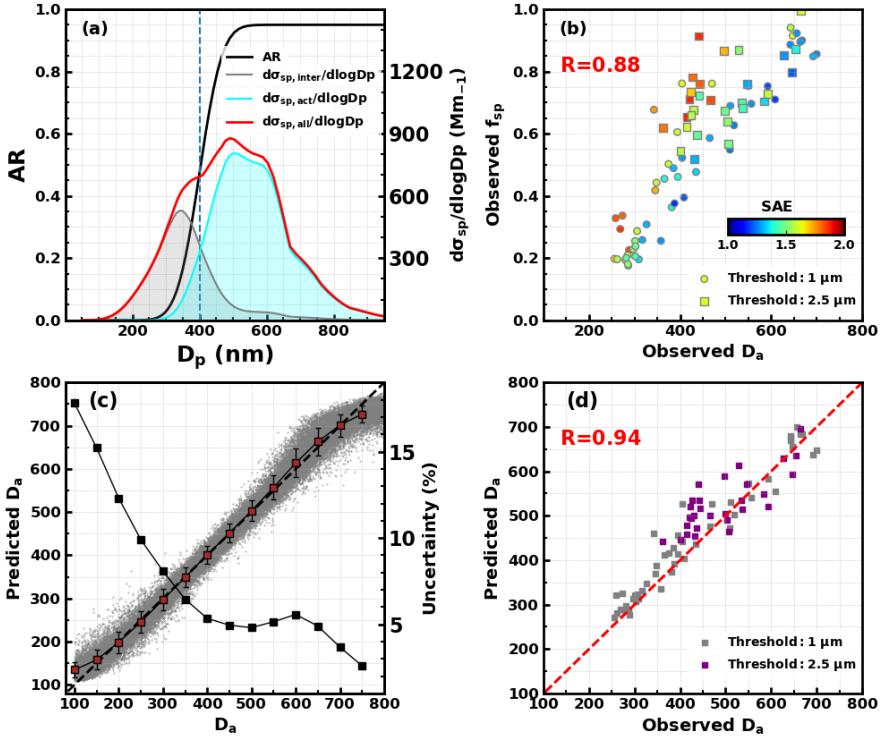

Figure 1. **(a)**The typical shape of size-resolved aerosol activation ratio (AR) curve produced using the function of Eq.2, with the Da of 400 nm, the MAF of 0.95 and the σ of 30, and the average PNSD observed in the North China Plain from six campaigns (Kuang et al., 2018) and the AR curve was used to simulate an example of the size-resolved aerosol scattering (σ_{sp}) distributions of interstitial and activated aerosols at 525 nm; **(b)** Relations between observed D_a and f_{sp} during the AQ-SOFAR campaign using 1 and 2.5 μm as the threshold of interstital aerosols, with the scatter points are colored with corresponding SAE of total dry state PM_1 aerosols. **(c)** Comparisons of all prescribed D_a and predicted $D_a$values represented by scatter points, they are further binned with interval of 50 nm, averages and standard deviations represented by purple squares and their error bars, black squares represent relative uncertainty of the right axis at each bin; **(d)** The comparisons of $D_a$retrieved using activation ratio observations and those predicted using scattering observations as inputs of the trained model, dashed lines represent 1:1 lines.

180 If we focus on PM_1 of the total dry aerosol population (the reasoning for this is discussed in Sect.
181 S1 of the supplement), the scattering fraction of interstitial aerosols in the total dry PM_1 population,
182 defined as $f_{sp} = \sigma_{sp,PM_1,inter}(dry, 525\ nm)/\sigma_{sp,PM_1,all}(dry, 525\ nm)$, where
183 $\sigma_{sp,PM_1,inter}(dry, 525\ nm)$ is the scattering coefficient of PM_1 interstitial aerosols in a dry state at a
184 wavelength of 525 nm, and $\sigma_{sp,PM_1,all}(dry, 525\ nm)$ is that of all PM_1 aerosols, is likely to be highly

https://doi.org/10.5194/egusphere-2024-2698
Preprint. Discussion started: 18 September 2024

correlated with D_a. Generally, the larger the D_a, the higher the f_{sp}. This relationship was directly confirmed using D_a and the scattering properties of dry PM_1 interstitial and total aerosols during the AQ-SOFAR campaign, as shown in Fig. 1b, that observed D_a correlates highly with observed f_{sp} (R=0.88). However, at a given D_a, f_{sp} can vary significantly, and these variations are closely related to the SAE of all dry PM_1 aerosols, which are mainly determined by aerosol size distribution. In fact, aside from the size distribution of the total aerosol population that determines SAE, the shape of the AR curve also plays a significant role in the variations of f_{sp}.

The nephelometer measures the aerosol scattering coefficient at three wavelengths, enabling direct measurements of the SAE for both the total dry-state PM_1 aerosols and the interstitial aerosols. Therefore, the relationship between f_{sp} and D_a can be further constrained by the SAE of interstitial and activated aerosols, as well as their wavelength dependence. This implies that a simple formulaic relationship between f_{sp} and D_a may not exist. However, the six scattering parameters $\sigma_{sp,PM_1,inter}(dry,\lambda)$—at 450 nm, 525 nm, 635 nm, and $\sigma_{sp,PM_1,all}(dry,\lambda)$ at 450 nm, 525 nm, 635 nm—contain both the f_{sp} information and the SAE characteristics of both aerosol groups, thus potentially be used to accurately retrieve D_a. Machine learning techniques, which are well-suited for handling complex relationships, can be applied to this problem.

This assumption was tested using Mie theory, based on aerosol size distributions sampled during six campaigns conducted in the North China Plain region (Kuang et al., 2018). For each aerosol size distribution, we randomly assumed different activation curves using Eq.2. The details of this simulation are provided in Sect. S2 of the supplement. The simulation pairs of these six scattering parameters and D_a were used to train a random forest model (Kuang et al., 2018). To preliminarily validate this approach, we randomly selected 75% of the simulated data points for training the model, while the remaining 25% were used for validation. The results, shown in Fig. 1c, indicate that this approach could retrieve D_a with an uncertainty of less than 10% for D_a larger than 250 nm, and even as low as ~6% for D_a larger than 350 nm. However, the uncertainty increases as D_a decreases, particularly for D_a smaller than 250 nm. The larger uncertainty at smaller D_a is due to the fact that aerosols smaller than 250 nm typically contribute less than 10% to total scattering in the dry state, making f_{sp} less sensitive to variations in D_a. This issue becomes more pronounced when D_a is less than 100 nm, as aerosols smaller than 150 nm generally contribute negligibly to total aerosol scattering [Kuang et al., 2018]. This method was further validated using observations from the AQ-SOFAR campaign. In this validation, D_a values were first predicted using aerosol scattering observations with

https://doi.org/10.5194/egusphere-2024-2698
Preprint. Discussion started: 18 September 2024

the trained model and then compared with D_a values retrieved from size-resolved AR measurements, as shown in Fig. 1d. It should be noted that the impactor operates in a sequence of PM_1, $PM_{2.5}$, TSP, and then back to PM_1, with the flow alternating between a thermodenuder and bypass every 10 minutes for each inlet. To calculate size-resolved AR curves, we assumed that aerosol populations remained unchanged during the 30-minute period (based on comparisons between PM_1/$PM_{2.5}$ and TSP inlets), which can sometimes introduce significant uncertainties in the size-resolved AR calculations. When using $PM_{2.5}$ as the threshold, the much lower number concentrations of aerosols larger than 400 nm can introduce more uncertainty in D_a retrievals, partially explaining the lower performance in Fig. 1d when using the $PM_{2.5}$ threshold.

3.2 Method of observing Hygroscopicity of Activated Aerosols

Measuring the hygroscopicity κ of activated aerosols at the critical activation diameter D_a under varying supersaturations is challenging, not only due to technical limitations but also because of the inherent variability in D_a. Kuang et al. (2017) introduced a novel optical method for observing aerosol hygroscopicity by using the aerosol light scattering enhancement factor $f(RH)$ that associated with aerosol hygroscopic growth. This method is particularly suitable for the objectives outlined here. The method requires SAE and light scattering enhancement factors $f(RH)$ of activated aerosols as inputs, and retrieved κ can be termed as $\kappa_{act,f(RH)}$ which represents the overall hygroscopicity of activated aerosols and can be understood as the average κ of activated aerosols with the scattering contribution of each aerosol particle as the weight (Kuang et al., 2020). The scattering coefficients of activated aerosols at multiwavelength can be calculated as $\sigma_{sp,PM_1,act}(dry,\lambda) = \sigma_{sp,PM_1,all}(dry,\lambda) - \sigma_{sp,PM_1,inter}(dry,\lambda)$, therefore corresponding SAE can be obtained. The $f(RH)$ of activated aerosols at 525 nm can be calculated as the following:

$$f(RH)_{act} = \frac{\sigma_{sp,PM_1,all}(RH,525\ nm) - \sigma_{sp,PM_1,inter}(RH,525\ nm)}{\sigma_{sp,PM_1,all}(dry,525\ nm) - \sigma_{sp,PM_1,inter}(dry,525\ nm)}$$

During the AQ-SOFAR campaign, a humidified nephelometer system consisting of two nephelometers—one measuring aerosol scattering in the dry state and the other at a fixed RH of 84%—was placed downstream of the PM_1 impactor. This setup allows for the humidification of dry-state interstitial aerosols and total aerosol populations to a high RH (e.g., above 80%), facilitating the required measurements, therefore severs one choice. The Retrieved $\kappa_{act,f(RH)}$ under different D_a conditions are shown in Fig.2a, demonstrating significant variations in $\kappa_{act,f(RH)}$ and its variations

https://doi.org/10.5194/egusphere-2024-2698
Preprint. Discussion started: 18 September 2024

need to constrained. Also, the derived $\kappa_{act,f(RH)}$ are compared those estimated from aerosol chemical compositions measurements ($\kappa_{act,chem}$, details about calculation methods can refer to Kuang et al. (2020)), as shown in Fig.2b and in general agree. Note that the mass spectrometer could not identify all aerosol components, and assumptions about the mixing rule as well as densities of components would bring uncertainties (Kuang et al., 2021). The comparisons between effective supersaturations derived from size-resolved AR measurements as well as $\kappa_{act,chem}$ and from the optical method are shown in Fig.2c. On average, 0.002% of SS bias are observed due to the bias of D_a which associated more with assumptions made in D_a retrievals as previously discussed. As demonstrated by Kuang et al. (2024), for the fog case in the campaign, the threshold of 2.5 μm should be used, however, does not affect the comparisons here.

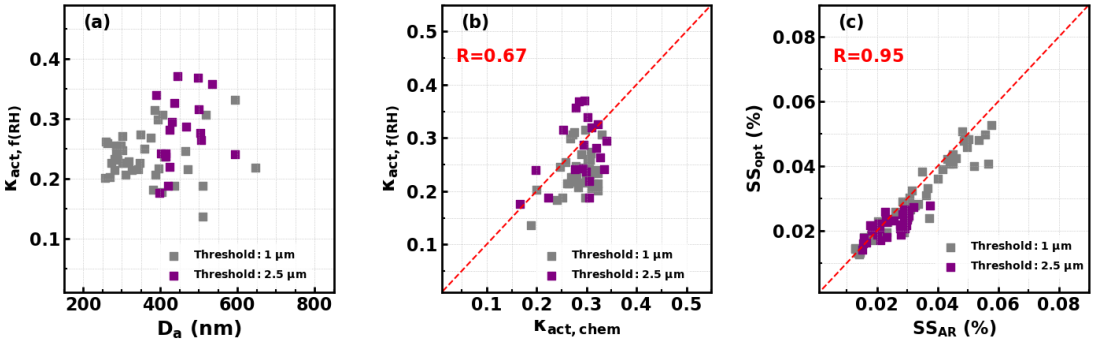

Figure 2. **(a)** Retrieved $\kappa_{act,f(RH)}$ under different D_a conditions; **(b)** Comparison between κ of activated aerosols retrieved from the optical method ($\kappa_{act,f(RH)}$) and estimated from aerosol chemical composition measurements ($\kappa_{act,chem}$) ;**(c)** Comparisons between effective supersaturations (SSs) derived from size-resolved AR measurements as well as $\kappa_{act,chem}$ (SS_{AR}) and from the optical measurements (SS_{opt}). Dashed red lines represent 1:1 lines.

Qiao et al. (2024) developed an advanced outdoor nephelometer system that measures aerosol dry scattering coefficients and scattering coefficients at nearly ambient RH without the need for humidifying the sample air by placing the entire nephelometer system in ambient air, with the instruments protected by a specially designed enclosure. This innovative design offers new insights into the hygroscopicity measurements of activated aerosols. Under cloud conditions, where the ambient RH is close to 100%, aerosol scattering under subsaturated conditions can be measured directly by applying heater.

https://doi.org/10.5194/egusphere-2024-2698
Preprint. Discussion started: 18 September 2024

3.3 Concept Design of the Advanced Optical System for Measuring Effective Supersaturations

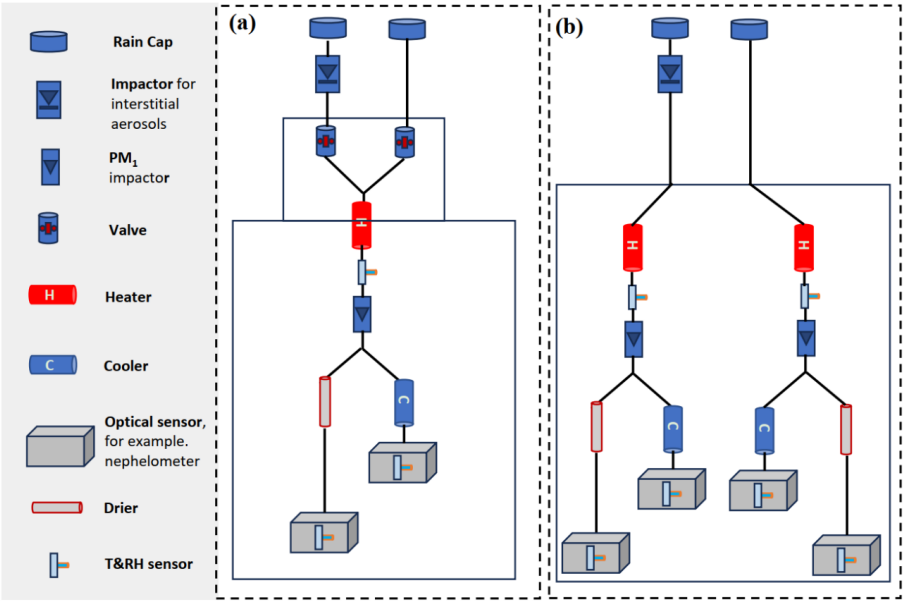

Figure 3. Concept design of the advanced optical system with different number of optical sensors, **(a)** using two nephelometers or other optical sensors; **(b)** using four nephelometers or other optical sensors.

Based on the proposed optical methods for measuring D_a and $\kappa_{act,f(RH)}$, a conceptual design for outdoor instruments capable of measuring effective supersaturation with relatively high time resolution can be envisioned, as shown in Fig. 3a. The aerosol-cloud sampling system includes two inlets: one equipped with a PM_1 or $PM_{2.5}$ impactor (depending on cloud type) to sample interstitial aerosols, and another with a TSP inlet to sample both interstitial aerosols and cloud/fog droplets. A PM_1 impactor is placed downstream of the inlet system, where the RH of the sample air is reduced to 70% (as discussed in Sect. S1 of the manuscript) through heater. Downstream of the PM1 impactor, the sample flow is split into two streams: one is further dried to an RH below 10% before aerosol scattering coefficients are measured by the "dry" nephelometer, and the other is passed through an intelligent cooler to ensure the sample RH in the "wet" nephelometer remains close to 90%. The sample air is automatically switched between the interstitial inlet and the TSP inlet at set intervals, such as one minute for each inlet, enabling minute-level measurements of effective supersaturations. While the nephelometer can output scattering measurements every second, reliable data can only be achieved at intervals of around 30 seconds (exact values can be determined through future testing) due to the residence time of aerosols in the nephelometer and potential light source instability. If four

https://doi.org/10.5194/egusphere-2024-2698
Preprint. Discussion started: 18 September 2024

nephelometers are available, a more advanced optical system can be designed (Fig. 3b) that does not require switching between the interstitial inlet and the TSP inlet. Instead, two nephelometers would be placed downstream of the interstitial inlet and two downstream of the TSP inlet, enabling higher time resolution effective supersaturation measurements. Other types of optical instruments exist that can achieve stable second-level aerosol scattering or extinction measurements with a stable laser light source [Moise et al., 2015; Zhou et al., 2020]. Therefore, with the development of suitable optical instruments, it may be possible to achieve second-level effective supersaturation measurements.

4. Discussions on Limitations and Advantages

The proposed theoretical framework enables simultaneous measurements of D_a and κ for activated aerosols, leveraging the high time resolution of optical instruments to potentially provide second-level measurements of supersaturation. However, several limitations should be discussed and might be improved upon: **(1) Shape of size-resolved AR curve:** Cloud chamber studies have shown that supersaturation fluctuations can lead to the coexistence of particles with the same critical supersaturation as both interstitial aerosols and cloud droplets (Shawon et al., 2021). This results in size-resolved AR curves deviate more from stepwise shape, a phenomenon also observed in some field measurements (Henning et al., 2004;Mertes et al., 2007). Despite this, a critical diameter D_a still exists, and such non-ideal curves can be treated a high standard deviation σ in the activation error function (Eq. 2), which does not fundamentally undermine the proposed framework, however, should be further checked for different cloud types. **(2) Measurement of κ:** Although the framework measures the overall κ of activated aerosols, the κ needed for supersaturation calculations is that of aerosols near D_a (κ_{D_a}). For D_a>~200 nm, the derived $\kappa_{act,f(RH)}$ can provide a first-order estimate of κ_{D_a}, based on observed size-dependent characteristics of κ values (Liu et al., 2014;Shen et al., 2021;Wang et al., 2024), though more comprehensive evaluations are needed. Additionally, κ measured under subsaturated conditions differs from that under supersaturated conditions (Tao et al., 2023) might also bring some uncertainties. However, as shown in Fig. S1b, a bias of 0.1 in κ only results in a 0.01% bias in supersaturation retrievals, making the first-order estimates of κ_{D_a} from optical measurements suitable for supersaturation observations. **(3) Limitations in D_a Retrievals:** Current techniques using aerosol scattering measurements at visible wavelengths (e.g., nephelometers) are reliable only for D_a>100 nm as shown in Fig.1a, limiting effective supersaturation measurements to less than 0.21% (assuming a typical κ of 0.3). This restriction makes the technique most applicable to fog and stratus or stratocumulus cloud measurements. However, incorporating scattering measurements at ultraviolet

https://doi.org/10.5194/egusphere-2024-2698
Preprint. Discussion started: 18 September 2024

wavelengths could improve sensitivity to smaller D_a and lower κ, enabling measurements in conditions with higher effective supersaturation and a broader range of cloud types in the future.

Despite these limitations, the proposed theoretical framework represents the first system capable of directly providing high time resolution measurements of effective supersaturations using a single instrument. This system is particularly well-suited for surface fog and mountain cloud observations, and when coupled with aerial vehicles, it could also be employed for measurements in aloft clouds. The system offers several advantages for cloud and fog measurements: **(1) High-Resolution Supersaturation Measurements:** The system can provide measurements of effective supersaturations at even a second-level resolution, making it feasible for observing effective supersaturation fluctuations and supporting investigations into fog and cloud evolution mechanisms. **(2) Long-Term Measurement Capability:** The optical measurements, such as those from the nephelometer system, are well-suited for long-term observations, making it possible to acquire climatological data on the variability of fogs and mountain clouds. **(3) Comprehensive Aerosol and Cloud Data:** In addition to measuring effective supersaturations, the system directly captures the scattering and hygroscopic properties of both interstitial and activated aerosols. With further algorithm development, it could also retrieve the number concentrations of available cloud condensation nuclei (CCN) at certain supersaturations, as well as cloud droplet number concentrations, based on previous studies that have observed CCN using optical methods (Tao et al., 2018a). **(4) Monitoring Aerosol Hygroscopic Behavior:** The system continuously monitors aerosol hygroscopic behavior under subsaturated conditions along with the corresponding optical properties. This allows for clear documentation of the formation and dissipation of fog/cloud events, as well as the variation in aerosol optical and hygroscopic properties. Overall, the datasets generated by this system are well-suited for in-depth investigations of cloud physics and aerosol-cloud interactions. This system has the potential to significantly advance fundamental research on clouds and fogs. However, further theoretical studies are needed to refine and optimize this type of system.

https://doi.org/10.5194/egusphere-2024-2698
Preprint. Discussion started: 18 September 2024

Financial Supports. This work is supported by National Natural Science Foundation of China (42175083, 42175127), and the Fundamental Research Funds for the Central Universities.

Competing interests. The authors declare that they have no conflict of interest.

Data Availability. All data presented in Figures of this manuscript are freely available at Kuang, Y. (2024), and more specific data will be made available on request.

Author contribution. YK conceived the theoretical framework and wrote the manuscript. JT, HX, L L, WX and WeX participated the field campaign and conducted measurements of aerosol chemical and physical properties. YS, PL, CZ reviewed and commented on the paper.

https://doi.org/10.5194/egusphere-2024-2698
Preprint. Discussion started: 18 September 2024

References

Abade, G. C., Grabowski, W. W., and Pawlowska, H.: Broadening of Cloud Droplet Spectra through Eddy Hopping: Turbulent Entraining Parcel Simulations, Journal of the Atmospheric Sciences, 75, 3365-3379, https://doi.org/10.1175/JAS-D-18-0078.1, 2018.

Abdul-Razzak, H., Ghan, S. J., and Rivera-Carpio, C.: A parameterization of aerosol activation: 1. Single aerosol type, Journal of Geophysical Research: Atmospheres, 103, 6123-6131, https://doi.org/10.1029/97JD03735, 1998.

Anderson, J. C., Beeler, P., Ovchinnikov, M., Cantrell, W., Krueger, S., Shaw, R. A., Yang, F., and Fierce, L.: Enhancements in Cloud Condensation Nuclei Activity From Turbulent Fluctuations in Supersaturation, Geophysical Research Letters, 50, e2022GL102635, https://doi.org/10.1029/2022GL102635, 2023.

Chandrakar, K. K., Cantrell, W., Chang, K., Ciochetto, D., Niedermeier, D., Ovchinnikov, M., Shaw, R. A., and Yang, F.: Aerosol indirect effect from turbulence-induced broadening of cloud-droplet size distributions, Proceedings of the National Academy of Sciences, 113, 14243-14248, doi:10.1073/pnas.1612686113, 2016.

Chandrakar, K. K., Cantrell, W., and Shaw, R. A.: Influence of Turbulent Fluctuations on Cloud Droplet Size Dispersion and Aerosol Indirect Effects, Journal of the Atmospheric Sciences, 75, 3191-3209, https://doi.org/10.1175/JAS-D-18-0006.1, 2018.

Chandrakar, K. K., Saito, I., Yang, F., Cantrell, W., Gotoh, T., and Shaw, R. A.: Droplet size distributions in turbulent clouds: experimental evaluation of theoretical distributions, Quarterly Journal of the Royal Meteorological Society, 146, 483-504, https://doi.org/10.1002/qj.3692, 2020.

Ditas, F., Shaw, R. A., Siebert, H., Simmel, M., Wehner, B., and Wiedensohler, A.: Aerosols-cloud microphysics-thermodynamics-turbulence: evaluating supersaturation in a marine stratocumulus cloud, Atmos. Chem. Phys., 12, 2459-2468, 10.5194/acp-12-2459-2012, 2012.

Gong, X., Wang, Y., Xie, H., Zhang, J., Lu, Z., Wood, R., Stratmann, F., Wex, H., Liu, X., and Wang, J.: Maximum Supersaturation in the Marine Boundary Layer Clouds Over the North Atlantic, AGU Advances, 4, e2022AV000855, https://doi.org/10.1029/2022AV000855, 2023.

Hammer, E., Gysel, M., Roberts, G. C., Elias, T., Hofer, J., Hoyle, C. R., Bukowiecki, N., Dupont, J. C., Burnet, F., Baltensperger, U., and Weingartner, E.: Size-dependent particle activation properties in fog during the ParisFog 2012/13 field campaign, Atmos. Chem. Phys., 14, 10517-10533, 10.5194/acp-14-10517-2014, 2014.

Henning, S., Bojinski, S., Diehl, K., Ghan, S., Nyeki, S., Weingartner, E., Wurzler, S., and Baltensperger, U.: Aerosol partitioning in natural mixed-phase clouds, Geophysical Research Letters, 31, https://doi.org/10.1029/2003GL019025, 2004.

Kaufman, Y. J., and Tanré, D.: Effect of variations in super-saturation on the formation of cloud condensation nuclei, Nature, 369, 45-48, 10.1038/369045a0, 1994.

Kuang, Y., Zhao, C., Tao, J., Bian, Y., Ma, N., and Zhao, G.: A novel method for deriving the aerosol hygroscopicity parameter based only on measurements from a humidified nephelometer system, Atmos. Chem. Phys., 17, 6651-6662, 10.5194/acp-17-6651-2017, 2017.

Kuang, Y., Zhao, C. S., Zhao, G., Tao, J. C., Xu, W., Ma, N., and Bian, Y. X.: A novel method for calculating ambient aerosol liquid water content based on measurements of a humidified nephelometer system, Atmospheric Measurement Techniques, 11, 2967-2982, 10.5194/amt-11-2967-2018, 2018.

Kuang, Y., He, Y., Xu, W., Zhao, P., Cheng, Y., Zhao, G., Tao, J., Ma, N., Su, H., Zhang, Y., Sun, J., Cheng, P., Yang, W., Zhang, S., Wu, C., Sun, Y., and Zhao, C.: Distinct diurnal variation in organic aerosol hygroscopicity and its relationship with oxygenated organic aerosol, Atmos. Chem. Phys., 20, 865-880, 10.5194/acp-20-865-2020, 2020.

Kuang, Y., Huang, S., Xue, B., Luo, B., Song, Q., Chen, W., Hu, W., Li, W., Zhao, P., Cai, M., Peng, Y., Qi, J., Li, T., Wang, S., Chen, D., Yue, D., Yuan, B., and Shao, M.: Contrasting effects of secondary

https://doi.org/10.5194/egusphere-2024-2698
Preprint. Discussion started: 18 September 2024

organic aerosol formations on organic aerosol hygroscopicity, Atmos. Chem. Phys., 21, 10375-10391, 10.5194/acp-21-10375-2021, 2021.
Kuang, Y., Xu, W., Tao, J., Luo, B., Liu, L., Xu, H., Xu, W., Xue, B., Zhai, M., Liu, P., and Sun, Y.: Divergent Impacts of Biomass Burning and Fossil Fuel Combustion Aerosols on Fog-Cloud Microphysics and Chemistry: Novel Insights From Advanced Aerosol-Fog Sampling, Geophysical Research Letters, 51, e2023GL107147, https://doi.org/10.1029/2023GL107147, 2024.
Liu, H. J., Zhao, C. S., Nekat, B., Ma, N., Wiedensohler, A., van Pinxteren, D., Spindler, G., Müller, K., and Herrmann, H.: Aerosol hygroscopicity derived from size-segregated chemical composition and its parameterization in the North China Plain, Atmos. Chem. Phys., 14, 2525-2539, 10.5194/acp-14-2525-2014, 2014.
Lu, C., Liu, Y., Yum, S. S., Chen, J., Zhu, L., Gao, S., Yin, Y., Jia, X., and Wang, Y.: Reconciling Contrasting Relationships Between Relative Dispersion and Volume-Mean Radius of Cloud Droplet Size Distributions, Journal of Geophysical Research: Atmospheres, 125, e2019JD031868, https://doi.org/10.1029/2019JD031868, 2020.
Mazoyer, M., Burnet, F., Denjean, C., Roberts, G. C., Haeffelin, M., Dupont, J. C., and Elias, T.: Experimental study of the aerosol impact on fog microphysics, Atmos. Chem. Phys., 19, 4323-4344, 10.5194/acp-19-4323-2019, 2019.
Mertes, S., Verheggen, B., Walter, S., Connolly, P., Ebert, M., Schneider, J., Bower, K. N., Cozic, J., Weinbruch, S., Baltensperger, U., and Weingartner, E.: Counterflow Virtual Impactor Based Collection of Small Ice Particles in Mixed-Phase Clouds for the Physico-Chemical Characterization of Tropospheric Ice Nuclei: Sampler Description and First Case Study, Aerosol Science and Technology, 41, 848-864, 10.1080/02786820701501881, 2007.
Petters, M. D., and Kreidenweis, S. M.: A single parameter representation of hygroscopic growth and cloud condensation nucleus activity, Atmospheric Chemistry and Physics, 7, 1961-1971, 2007.
Prabhakaran, P., Shawon, A. S. M., Kinney, G., Thomas, S., Cantrell, W., and Shaw, R. A.: The role of turbulent fluctuations in aerosol activation and cloud formation, Proceedings of the National Academy of Sciences, 117, 16831-16838, 10.1073/pnas.2006426117, 2020.
Qiao, H., Kuang, Y., Yuan, F., Liu, L., Zhai, M., Xu, H., Zou, Y., Deng, T., and Deng, X.: Unlocking the Mystery of Aerosol Phase Transitions Governed by Relative Humidity History Through an Advanced Outdoor Nephelometer System, Geophysical Research Letters, 51, e2023GL107179, https://doi.org/10.1029/2023GL107179, 2024.
Rose, D., Gunthe, S. S., Mikhailov, E., Frank, G. P., Dusek, U., Andreae, M. O., and Pöschl, U.: Calibration and measurement uncertainties of a continuous-flow cloud condensation nuclei counter (DMT-CCNC): CCN activation of ammonium sulfate and sodium chloride aerosol particles in theory and experiment, Atmos. Chem. Phys., 8, 1153-1179, 10.5194/acp-8-1153-2008, 2008.
Saito, I., Gotoh, T., and Watanabe, T.: Broadening of Cloud Droplet Size Distributions by Condensation in Turbulence, Journal of the Meteorological Society of Japan. Ser. II, 97, 867-891, 10.2151/jmsj.2019-049, 2019.
Saliba, G., Bell, D. M., Suski, K. J., Fast, J. D., Imre, D., Kulkarni, G., Mei, F., Mülmenstädt, J. H., Pekour, M., Shilling, J. E., Tomlinson, J., Varble, A. C., Wang, J., Thornton, J. A., and Zelenyuk, A.: Aircraft measurements of single particle size and composition reveal aerosol size and mixing state dictate their activation into cloud droplets, Environmental Science: Atmospheres, 3, 1352-1364, 10.1039/D3EA00052D, 2023.
Sanchez, K. J., Russell, L. M., Modini, R. L., Frossard, A. A., Ahlm, L., Corrigan, C. E., Roberts, G. C., Hawkins, L. N., Schroder, J. C., Bertram, A. K., Zhao, R., Lee, A. K. Y., Lin, J. J., Nenes, A., Wang, Z., Wonaschütz, A., Sorooshian, A., Noone, K. J., Jonsson, H., Toom, D., Macdonald, A. M., Leaitch, W. R., and Seinfeld, J. H.: Meteorological and aerosol effects on marine cloud microphysical properties, Journal of Geophysical Research: Atmospheres, 121, 4142-4161, https://doi.org/10.1002/2015JD024595, 2016.

https://doi.org/10.5194/egusphere-2024-2698
Preprint. Discussion started: 18 September 2024

Sanchez, K. J., Roberts, G. C., Saliba, G., Russell, L. M., Twohy, C., Reeves, J. M., Humphries, R. S., Keywood, M. D., Ward, J. P., and McRobert, I. M.: Measurement report: Cloud processes and the transport of biological emissions affect southern ocean particle and cloud condensation nuclei concentrations, Atmos. Chem. Phys., 21, 3427-3446, 10.5194/acp-21-3427-2021, 2021.

Sardina, G., Picano, F., Brandt, L., and Caballero, R.: Continuous Growth of Droplet Size Variance due to Condensation in Turbulent Clouds, Physical Review Letters, 115, 184501, 10.1103/PhysRevLett.115.184501, 2015.

Seinfeld, J., and Pandis, S.: Atmospheric Chemistry and Physics: From Air Pollution to Climate Change, Third Edition, 2016.

Seinfeld, J. H., Bretherton, C., Carslaw, K. S., Coe, H., DeMott, P. J., Dunlea, E. J., Feingold, G., Ghan, S., Guenther, A. B., Kahn, R., Kraucunas, I., Kreidenweis, S. M., Molina, M. J., Nenes, A., Penner, J. E., Prather, K. A., Ramanathan, V., Ramaswamy, V., Rasch, P. J., Ravishankara, A. R., Rosenfeld, D., Stephens, G., and Wood, R.: Improving our fundamental understanding of the role of aerosol−cloud interactions in the climate system, Proceedings of the National Academy of Sciences, 113, 5781-5790, 10.1073/pnas.1514043113, 2016.

Shaw, R. A., Cantrell, W., Chen, S., Chuang, P., Donahue, N., Feingold, G., Kollias, P., Korolev, A., Kreidenweis, S., Krueger, S., Mellado, J. P., Niedermeier, D., and Xue, L.: Cloud–Aerosol–Turbulence Interactions: Science Priorities and Concepts for a Large-Scale Laboratory Facility, Bulletin of the American Meteorological Society, 101, E1026-E1035, https://doi.org/10.1175/BAMS-D-20-0009.1, 2020.

Shawon, A. S. M., Prabhakaran, P., Kinney, G., Shaw, R. A., and Cantrell, W.: Dependence of Aerosol-Droplet Partitioning on Turbulence in a Laboratory Cloud, Journal of Geophysical Research: Atmospheres, 126, e2020JD033799, https://doi.org/10.1029/2020JD033799, 2021.

Shen, C., Zhao, C., Ma, N., Tao, J., Zhao, G., Yu, Y., and Kuang, Y.: Method to Estimate Water Vapor Supersaturation in the Ambient Activation Process Using Aerosol and Droplet Measurement Data, Journal of Geophysical Research: Atmospheres, 0, 10.1029/2018JD028315, 2018.

Shen, C., Zhao, G., Zhao, W., Tian, P., and Zhao, C.: Measurement report: aerosol hygroscopic properties extended to 600 nm in the urban environment, Atmos. Chem. Phys., 21, 1375-1388, 10.5194/acp-21-1375-2021, 2021.

Siebert, H., and Shaw, R. A.: Supersaturation Fluctuations during the Early Stage of Cumulus Formation, Journal of the Atmospheric Sciences, 74, 975-988, https://doi.org/10.1175/JAS-D-16-0115.1, 2017.

Tao, J., Zhao, C., Kuang, Y., Zhao, G., Shen, C., Yu, Y., Bian, Y., and Xu, W.: A new method for calculating number concentrations of cloud condensation nuclei based on measurements of a three-wavelength humidified nephelometer system, Atmos. Meas. Tech., 11, 895-906, 10.5194/amt-11-895-2018, 2018a.

Tao, J., Zhao, C., Ma, N., and Kuang, Y.: Consistency and applicability of parameterization schemes for the size-resolved aerosol activation ratio based on field measurements in the North China Plain, Atmospheric Environment, 173, 316-324, https://doi.org/10.1016/j.atmosenv.2017.11.021, 2018b.

Tao, J., Kuang, Y., Luo, B., Liu, L., Xu, H., Ma, N., Liu, P., Xue, B., Zhai, M., Xu, W., Xu, W., and Sun, Y.: Kinetic Limitations Affect Cloud Condensation Nuclei Activity Measurements Under Low Supersaturation, Geophysical Research Letters, 50, e2022GL101603, https://doi.org/10.1029/2022GL101603, 2023.

Wainwright, C., Chang, R. Y.-W., and Richter, D.: Aerosol Activation in Radiation Fog at the Atmospheric Radiation Program Southern Great Plains Site, Journal of Geophysical Research: Atmospheres, 126, e2021JD035358, https://doi.org/10.1029/2021JD035358, 2021.

Wang, Y., Li, J., Fang, F., Zhang, P., He, J., Pöhlker, M. L., Henning, S., Tang, C., Jia, H., Wang, Y., Jian, B., Shi, J., and Huang, J.: In-situ observations reveal weak hygroscopicity in the Southern Tibetan Plateau: implications for aerosol activation and indirect effects, npj Climate and Atmospheric Science, 7, 77, 10.1038/s41612-024-00629-x, 2024.

https://doi.org/10.5194/egusphere-2024-2698
Preprint. Discussion started: 18 September 2024

513 Yang, F., McGraw, R., Luke, E. P., Zhang, D., Kollias, P., and Vogelmann, A. M.: A new approach
514 to estimate supersaturation fluctuations in stratocumulus cloud using ground-based remote-sensing
515 measurements, Atmos. Meas. Tech., 12, 5817-5828, 10.5194/amt-12-5817-2019, 2019.
516 Yum, S. S., Hudson, J. G., and Xie, Y.: Comparisons of cloud microphysics with cloud condensation
517 nuclei spectra over the summertime Southern Ocean, Journal of Geophysical Research: Atmospheres,
518 103, 16625-16636, https://doi.org/10.1029/98JD01513, 1998.
519 Zíková, N., Pokorná, P., Makeš, O., Sedlák, P., Pešice, P., and Ždímal, V.: Activation of atmospheric
520 aerosols in fog and low clouds, Atmospheric Environment, 230, 117490,
521 https://doi.org/10.1016/j.atmosenv.2020.117490, 2020.

522